16th International Symposium on Origin of Matter and Evolution of Galaxies (OMEG16), Ha Noi, Viet Nam, October 25-28, 2022

3 min. video

Direct triple-α process in non-adiabatic approach

M. Katsuma

Advanced mathematical institute, Osaka City University, Japan
Institut d'Astronomie et d'Astrophysique, Université Libre de Bruxelles, Belgium

Triple-α reaction rates have been determined well with the sequential process via the narrow resonances. However, direct triple-α process at off-resonant energies still remains in unsolved problems. In the present report, the direct process is estimated with non-adiabatic Faddeev HHR. In a result, the direct 3α contribution is found to be 10^{-15}_10^{-3} pb order in photo-disintegration of ^{12}C(2^+_1→0^+) for 0.15 < *E* < 0.35 MeV. This is far below the predicted values of the recent adiabatic models. In spite of the large difference, the derived rates are illustrated to be concordant with NACRE at the helium burning temperatures.

1.1 Introduction

Triple-α reaction plays an important role in nucleosynthesis heavier than ^{12}C, because no stable nuclei exist in mass number A=5 and A=8 [1,2]. Followed by ^{12}C(α,γ)^{16}O [3], triple-α reaction controls C/O ratio at the end of helium burning phase in stars, and it affects up to the nucleosynthesis in *e.g.* supernova explosion.

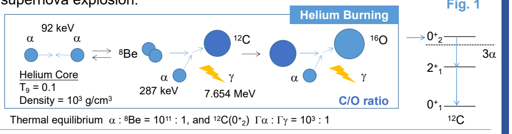

Fig. 1

Thermal equilibrium α : ^{8}Be = 10^{11} : 1, and ^{12}C(0^+_2) Γα : Γγ = 10^3 : 1

1.4 Present Report

I estimate **direct triple-α process** with non-adiabatic Faddeev **HHR***, and I calculate the 3α reaction rates at the helium burning temperatures. After I review Faddeev HHR used in the present report, I discuss the difference between the non-adiabatic and adiabatic approaches. To show the long-range Coulomb coupling effects, I also demonstrate calculations without screening.

1.2 Sequential process

Triple-α reaction via the resonances, (Fig. 1)

- In contrast to ^{12}C(α,γ)^{16}O, triple-α reaction is currently well-understood through the experimental studies of the 0^+_2 state in ^{12}C (E_R = 0.379 MeV). E_R is the c.m. energy with respect to the 3α threshold in ^{12}C.
- *i.e.* the reaction rates have been determined successfully with the **sequential process** via the narrow resonances. (*e.g.* [4,5])
- Pioneering work: **CF88** [6], Nomoto (1985) [7]

Standard Evaluated Reaction Rates

NACRE (1999) [5]

- Experimental update from CF88, based on Nomoto (1985) [7], Langanke (1986) [8].
- \+ Microscopic calculation of $J^\pi = 2^+_2$ by Descouvemont & Baye (1987) [9].
- ^{8}Be is assumed to be bound. The reaction proceeds via two resonances: ^{8}Be (0^+_1), ^{12}C (0^+_2).
- The adopted experimental values are
  - ^{8}Be (0^+_1): E_R = 0.092 MeV, Γ = 5.6 eV,
  - ^{12}C (0^+_2): E_R = 0.379 MeV, Γ = 8.3 eV, Γ_γ = 3.7 meV.

Recent experimental progress about the sequential process is found in [4].

1.3 Direct triple-α process

Triple-α reaction from 3α continuum states

3α Continuum Problem

- Relax the continuum states of ^{8}Be
- Not via the resonances
- This direct 3α process is generally expected to be *very* slow, because three α-particles almost simultaneously collide and fuse into a ^{12}C nucleus.

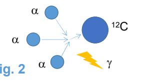

Fig. 2

Adiabatic approach

- Formulae in hyper-spherical coordinates have been applied to tackle the 3α continuum problem. (*e.g.* [10])
- Recently, the Coulomb Modified Faddeev (**CMF**) method [11] and adiabatic channel function (**ACF**) expansion method [12] may have achieved the successful progress quantitatively.
- However, non-adiabatic quantum-mechanical description at off-resonant energies still seems to remain in unsolved problems.

Non-adiabatic approach

- Faddeev Hyperspherical Harmonics and *R*-matrix (**HHR**) expansion method has been also performed in [13,14,15].

2.1 Faddeev HH expansion

Three-body Schrödinger equation: $(H_{3\alpha} - E)\Psi = 0$ (1)

- Faddeev equations, consisting of three components,

$$\left\{\begin{array}{lcl} \left[\hat{T}_{(1)} + (\hat{V}_{31} + \hat{V}_{3\alpha}) - E\right]\Psi_{(1)} &=& -\hat{V}_{31}\Psi_{(2)} - \hat{V}_{31}\Psi_{(3)} \\ \left[\hat{T}_{(2)} + (\hat{V}_{23} + \hat{V}_{3\alpha}) - E\right]\Psi_{(2)} &=& -\hat{V}_{23}\Psi_{(3)} - \hat{V}_{23}\Psi_{(1)} \\ \left[\hat{T}_{(3)} + (\hat{V}_{12} + \hat{V}_{3\alpha}) - E\right]\Psi_{(3)} &=& -\hat{V}_{12}\Psi_{(1)} - \hat{V}_{12}\Psi_{(2)} \end{array}\right. \qquad (2)$$

- Three identical sets of equations are found, because of the symmetric 3α system. Third component is rewritten as

$$\left[-\frac{\hbar^2}{2\mu_{12}}\nabla^2_{\bar{x}_3} - \frac{\hbar^2}{2\mu_{(12)3}}\nabla^2_{\bar{y}_3} + \hat{V}_{sym}\right]\Psi_{lm} = E\,\Psi_{lm}, \qquad \hat{V}_{sym} = \sum_{i<j}^{3} V_{\alpha\alpha}(\boldsymbol{r}_{ij}) + V_{3\alpha} \qquad (3)$$

3α interaction

α+α interaction

Coupled-channel (CC) equations with hyper-radial wavefunctions:

$$\begin{aligned} \left[T_\gamma + U^l_{\gamma\gamma}(\rho) - \epsilon\right]\chi^l_\gamma(\rho) &= -\sum_{\gamma'\neq\gamma} U^l_{\gamma'\gamma}(\rho)\chi^l_{\gamma'}(\rho) \\ T_\gamma &= \frac{d^2}{d\rho^2} - \frac{(K+3/2)(K+5/2)}{\rho^2} \\ U^l_{\gamma'\gamma} &= -\frac{2m_N}{\hbar^2}V^l_{\gamma'\gamma}(\rho), \\ \epsilon &= -\frac{2m_N}{\hbar^2}E. \end{aligned} \qquad (5)$$

Translate Jacobi coordinates into hyper-spherical coordinates

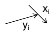

$$\rho^2 = x_i^2 + y_i^2, \qquad \theta_i = \arctan\left(\frac{x_i}{y_i}\right) \qquad (4)$$

The coordinates are different from CMF.

- Introducing hyper-angular momentum *K*, I obtain the *ordinary* CC equations for inelastic scattering. *e.g.* [16,17] (if *L*= *K*+3/2).

Basis functions:

Functions of ρ and Ω_5 are separated.

$$\begin{aligned} \Psi_{lm} &= \rho^{-5/2}\sum_{\gamma n} c^n_\gamma \varphi^K_n(\rho)\Phi^\gamma_{lm}(\Omega_5) \\ \chi^l_\gamma(\rho) &= \sum_n c^n_\gamma \varphi^K_n(\rho). \qquad \Phi^\gamma_{lm}(\Omega_5) = \phi^{l_{x_3}l_{y_3}}_K(\theta_3)\left[Y_{l_{x_3}}(\hat{\boldsymbol{x}}_3)\otimes Y_{l_{y_3}}(\hat{\boldsymbol{y}}_3)\right]_{lm} \\ \phi^{l_{x_3}l_{y_3}}_K(\theta_3) &= N^{l_{x_3}l_{y_3}}_{n_\theta}(\sin\theta_3)^{l_{x_3}}(\cos\theta_3)^{l_{y_3}}G_{n_\theta}(a,b;\sin^2\theta_3) \end{aligned} \qquad (6)$$

Hyper-harmonic functions

Hyper-radial wave functions

Normalization

Jacobi polynomials

- The final results are independent of the adopted $\varphi^K_n(\rho)$, if a large number of basis functions are used so as to expand well the wave functions.

2.2 *R*-matrix expansion

CC equations of Eq.(5): $(\boldsymbol{T}+\boldsymbol{U})\boldsymbol{X} = \epsilon\boldsymbol{X}$ (7)

- Matrix diagonalization, matrix size: (8,800 x 8,800) for 0^+ in ^{12}C
- Eigenstates, $E(l^+_i) = -\frac{\hbar^2}{2m_N}\epsilon_i, \quad \chi^l_{\gamma i}(\rho) = \sum_n c^n_{\gamma i}\varphi^K_n(\rho)$ (8)
  - $E(l^+_i)$ < 0, Bound states, $\chi^l_{\gamma i}(\rho) \to N^l_{\gamma i}W_{-\eta_\gamma,K+2}(2\kappa\rho)$ (9)
    N: normalization constants, *W*: Whitterker functions
  - $E(l^+_i)$ > 0, Resonances corresponding to low-lying levels & mathematically orthogonal states without specific interpretation in physics.

R-matrix expansion: Continuum states with scattering boundary condition are expanded with the resultant eigenfunctions.

Expansion of interior scattering waves:

a_c : channel radius

$$\chi^{l\,in}_{\alpha\beta}(k,\rho) = \sum_i A_{i\beta}(k)\chi^l_{\alpha i}(\rho) \qquad (10)$$

$$A_{i\beta}(k) = \frac{\hbar^2}{2m_N}\frac{1}{E(l^+_i)-E}\sum_\gamma \chi^l_{\gamma i}(a_c)\left[H^{-\prime}_{K+3/2}(\eta_\gamma;ka_c)\delta_{\gamma\beta} - S^l_{\gamma\beta}(E,a_c)H^{+\prime}_{K+3/2}(\eta_\gamma;ka_c)\right] \qquad (11)$$

S-matrix

Incoming Coulomb function

Outgoing Coulomb function

- *S*-matrix is defined by *R*-matrix,

$$\begin{aligned} S^l_{\alpha\beta}(E,a_c) &= [Z^*_{\alpha\beta}(E,a_c)]^{-1}Z_{\alpha\beta}(E,a_c), && (12) \\ Z_{\alpha\beta}(E,a_c) &= H^-_{K+3/2}(\eta_\alpha;ka_c)\delta_{\alpha\beta} - a_cR^l_{\alpha\beta}(E,a_c)H^{-\prime}_{K+3/2}(\eta_\beta;ka_c) && (13) \\ R^l_{\alpha\beta}(E,a_c) &= \sum_i \frac{\tilde{\gamma}_{\alpha i}\tilde{\gamma}_{\beta i}}{E(l^+_i)-E} && (14) \end{aligned}$$

R-matrix

- Reduced width amplitudes are defined as $\tilde{\gamma}_{\alpha i} = \sqrt{\frac{\hbar^2}{2m_Na_c}}\chi^l_{\alpha i}(a_c)$ (15)
- To include long-range Coulomb couplings, CC equations in the external region are solved numerically from ρ = a_c to ρ = ρ_m, $\chi^{l\,in}_{\alpha\beta}(k,a_c) \longrightarrow \chi^{l\,ext}_{\alpha\beta}(k,\rho)$. I use *R*-matrix propagation technique [13] to obtain the linearly-independent solutions.

Expansion by the linearly-independent waves:

$$\tilde{\chi}^l_{\gamma\gamma_0}(k,\rho) = \sum_{\gamma'} C_{\gamma'\gamma_0}(k)\chi^{l\,ext}_{\gamma\gamma'}(k,\rho) \qquad (16)$$

- The coefficients are obtained by matching to the asymptotic form of w.f.,

$$\tilde{\chi}^l_{\gamma\gamma_0}(k,\rho) \to \frac{i}{2}\left[I^{(\gamma_0)}_{\gamma,K+3/2}(\eta_\gamma;k\rho_m) - \sum_{\gamma'} S^l_{\gamma'\gamma_0}(E)O^{(\gamma')}_{\gamma,K+3/2}(\eta_\gamma;k\rho_m)\right] \qquad (17)$$

- Coupled-Coulomb waves [17]: $O^{(\gamma')}_{\gamma,K+3/2}(\eta_\gamma;k\rho) = a^{(\gamma')}_\gamma(k,\rho)H^+_{\gamma,K+3/2}(\eta_\gamma;k\rho), \quad I = O^*$ (18)
  \+ screening, $a^{(\gamma')}_\gamma \to \delta_{\gamma\gamma'}$ Effective, if the off-diagonal part of Coulomb coupling potentials is relatively small at a matching radius ρ_m, compared with *E*. (*e.g.*[16])
- Interior scattering waves including long-range Coulomb couplings are obtained as

$$\begin{aligned} \tilde{\chi}^{l\,in}_{\gamma\gamma_0}(k,\rho) &= \sum_{\gamma'} C_{\gamma'\gamma_0}(k)\chi^{l\,in}_{\gamma\gamma'}(k,\rho) \leftarrow \text{Eq.(10)} \qquad D_{i\gamma_0}(k) \equiv \sum_{\gamma'} C_{\gamma'\gamma_0}(k)A_{i\gamma'}(k) \\ &= \sum_i D_{i\gamma_0}(k)\chi^l_{\gamma i}(\rho) \qquad \chi^l_{\gamma i}(\rho) = \sum_n c^n_{\gamma i}\varphi^K_n(\rho) \end{aligned} \qquad (19)$$

Continuum states

Eigenfunctions, Eq.(8)

Arbitrary orthogonal functions

- B(E2) strength between 0^+ continuum states and 2^+_1 are calculated with Eqs. (8), (16) and (19). Quadruple precision is required to execute stable calculations.

B(E2) strength:

$$\frac{dB(E2;0^+\to 2^+_1)}{dE} = \frac{5e^2}{2\pi\hbar v}\sum_{\gamma_0}\left|\sum_{\gamma'\gamma} M^{2^+_10^+}_{\gamma'\gamma\gamma_0}(k)\left(f^x_{\gamma'\gamma}\zeta_x + f^y_{\gamma'\gamma}\zeta_y\right)\right|^2 \qquad (20)$$

Hyper-angle part

Hyper-radial part

$$M^{2^+_10^+}_{\gamma'\gamma\gamma_0}(k) = M^{2^+_10^+\,Int}_{\gamma'\gamma\gamma_0}(k) + M^{2^+_10^+\,Ext}_{\gamma'\gamma\gamma_0}(k) \qquad (21)$$

- Internal component, $M^{2^+_10^+\,Int}_{\gamma'\gamma\gamma_0}(k) = i^K\sum_i D_{i\gamma_0}(k)\int_0^{a_c}\chi^{2^+_1}_{\gamma'1}(\rho)\chi^{0^+}_{\gamma i}(\rho)\rho^2d\rho$ (22)
- External component, $M^{2^+_10^+\,Ext}_{\gamma'\gamma\gamma_0}(k) = i^K\int_{a_c}^\infty \chi^{2^+_1}_{\gamma'1}(\rho)\tilde{\chi}^{0^+}_{\gamma\gamma_0}(k,\rho)\rho^2d\rho$ (23)

Photo-disintegration cross sections: $\sigma_g(E) = \frac{4\pi^3}{75}\left(\frac{E_g}{\hbar c}\right)^3\frac{1}{5}\frac{dB(E2;0^+\to 2^+_1)}{dE}$ (24)

Reaction rates:

$$\begin{aligned} R_{3\alpha}(E) &= N_A^2\frac{480\pi}{(\mu_{12}\mu_{(12)3})^{3/2}}\frac{\hbar^3}{c^2}\frac{E_g^2}{E^2}\sigma_g(E) && (25) \\ \langle R_{3\alpha}\rangle &= \frac{1}{2}\frac{1}{(k_BT)^3}\int_0^\infty R_{3\alpha}(E)E^2e^{-E/(k_BT)}dE && (26) \end{aligned}$$

3.1 B(E2; 0^+→2^+_1) strength

The calculated results shown here are irrelevant to a group of [13]. To avoid confusion, my calculations are labeled with **HHR***. (**S**tudy of **T**riple-**α** **R**eaction)

HHR*

- Identical to [13] for *E* > 0.15 MeV.
- Resonance at 0.3795 MeV
  - α+^{8}Be, Sequential process (Fig.1)
- Other off-resonant energies
  - 3α, no specific shape, Direct triple-α process (Fig.2)
- I adopt two types of α+α interaction. (Panel 4.1) However, the calculated results do not strongly depend on the interactions.

Table 1

E(MeV)	0.20	0.30	0.3795	0.40	0.50
d_{scrn}(%)	0.62	0.31	0.32	0.30	0.07

- Coulomb couplings for ρ > 800 fm seem to be negligible. (Table 1)
  - Screening: 800 fm
  - Matching: 3000 fm

$$d_{scrn} = \left|\frac{dB(E2)/dE_{srcn} - dB(E2)/dE}{dB(E2)/dE}\right| \times 100 \qquad (27)$$

(screen) (no screen)

- *E* < 0.15 MeV: *Under consideration*
  - Screening of 800 fm is adopted.

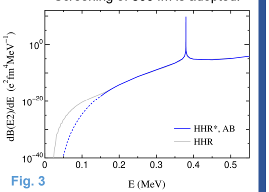

Fig. 3

3.2 Photo-disintegration of ^{12}C(2^+_1→0^+)

HHR*

- The resonance, bound state, and continuum states are all expanded by the 3α basis functions.
- α+^{8}Be feature is deduced without any assumption. (Panel 4.2)
- Direct 3α process: σ_g are in 10^{-15}_10^{-3} pb order for 0.15 < *E* < 0.35 MeV. These are much smaller than CMF and ACF.

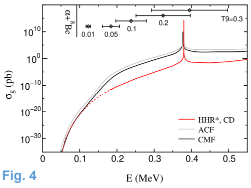

Fig. 4

CMF [11]

- CMF has been developed below the three-body threshold, *e.g.* low-energy p+d reactions.
- The internal motion of ^{8}Be in break-up channels is assumed to be localized within a certain range, and a cut-off procedure of non-local integral kernels is adopted.

ACF [12]

- ACF has the feature of α+^{8}Be for ρ < 150 fm and 3α for the large ρ.
- The resonance and bound states are expanded with the adiabatic basis.
- The complex absorbing potential does not make a large effect on σ_g, as well as screening.
- Most of the differences between ACF and HHR* seem to stem from the assumed internal adiabatic feature.

3.3 Comparison between reaction rates

- The derived reaction rates are consistent with NACRE for 0.08 < T_9 < 3, including the important helium burning temperatures. (Figs. 5 and 6)
- In contrast, the rates below T_9 = 0.07 may have to be studied further.
- The present result is reduced by 10^{-4} at T_9 = 0.05, because σ_g are reduced from ACF and CMF with the sequential process at *E* = 0.18 MeV in Fig. 4.
- Due to the strong influence of 0^+_2, the difference in σ_g for *E* > 0.2 MeV cannot be found in the reaction rates.
- Astrophysical impact of the difference in the theoretical rates has been expected to be small, because the difference is found before helium burning temperatures.

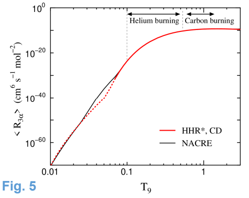

Fig. 5

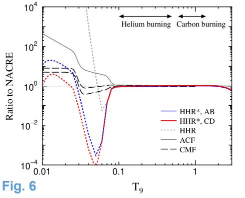

Fig. 6

4.1 α+α interaction & ^{8}Be

$$V^N_{\alpha\alpha}(\bar{x}_i) = (V_{c0}\mathbf{P_0} + V_{c2}\mathbf{P_2})e^{-(\bar{x}_i/a)^2} + V_0e^{-(\bar{x}_i/b)^2} \qquad (28)$$

Pauli repulsion Nucl. attraction

Table 2

	V_{c0} (MeV)	V_{c2} (MeV)	a (fm)	V_0 (MeV)	b (fm)	J_v(MeV fm^3)
AB	125.	20.	1.53	−30.18	2.85	243
CD	295.45	197.8	1.57	−118.7	2.16	416

- AB: shallow [18,10,13]
- CD: core+deep, folding potentials [19,20], reproducing phase shifts & α-width of 0^+_1

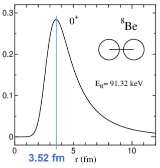

Fig. 8

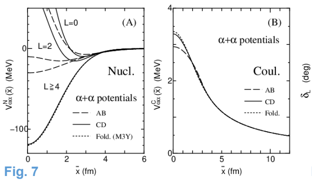

Fig. 7

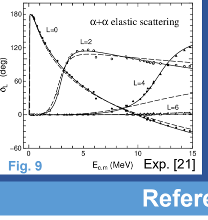

Fig. 9 Exp. [21]

4.2 Density distribution function of ^{12}C

Three peaks in 0^+_2 (HHR*, CD) **Equilateral triangle in 2^+_1** (HHR*, CD)

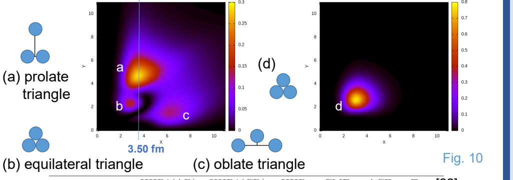

(a) prolate triangle

(d)

(b) equilateral triangle

(c) oblate triangle

Fig. 10

Table 3

	HHR*(AB)	HHR*(CD)	HHR	CMF	ACF	Exp.[22]
$E(0^+_2)$ (MeV)	0.3795	0.3796	0.380	0.379	0.379	0.379
$E(2^+_1)$ (MeV)	-2.838	-2.833	-2.875	-2.83	-2.836	-2.835
$E(0^+_1)$ (MeV)	-5.187	-7.213		-7.789	-9.242	-7.275
$R_{\rm rms}(0^+_2)$ (fm)	3.75	3.52		3.43	4.00	
$R_{\rm rms}(2^+_1)$ (fm)	2.46	2.46	2.459		2.40	
$R_{\rm rms}(0^+_1)$ (fm)	2.60	2.44			2.30	
$\Gamma_\alpha(0^+_2)$ (eV)	5.1	4.7		5.8	15.8	9.3
$\Gamma_\gamma(0^+_2)$ (meV)	4.3	6.5		2.2	9.57	3.81

5. Summary

In the present report, I have estimated the contribution of the direct triple-α process with non-adiabatic Faddeev HHR*, and I have shown the derived reaction rates at the helium burning temperatures.

- Described Faddeev HHR* expansion method.
- Discussed the difference between the non-adiabatic and adiabatic calculations.
- Demonstrated the calculations without screening.

HHR*

- ✲ Direct triple-α contribution is found to be 10^{-15}_10^{-3} pb order in the photo-disintegration cross sections of ^{12}C (2^+_1→0^+) for 0.15 < *E* < 0.35 MeV. This is far below the values predicted by ACF and CMF that include the assumed long resonant tail of 0^+_2, *i.e.* the sequential process. In spite of the large difference between the non-adiabatic and adiabatic cross sections, the derived reaction rates are found to be concordant with NACRE at the helium burning temperatures.
- ✲ The 0^+_2 state in ^{12}C is confirmed to have the dominant α+^{8}Be configuration in the density distribution function. *i.e.*, α+^{8}Be feature of the sequential process is deduced without any assumption. The calculated α- and γ-decay widths of 0^+_2 are comparable to the experimental data.
- ✲ The calculated results do not strongly depend on the adopted interactions.
- ✲ Coulomb couplings for ρ > 800 fm seem to be negligible at the energies corresponding to the helium burning temperatures.

Astrophysical impact of the direct triple-α process seems to be small, because of the strong influence of 0^+_2 in ^{12}C. It would have been, however, important for theoretical nuclear physicists to understand the off-resonant cross sections, non-adiabatically, and to examine how slow the direct process is at the temperatures relevant to stellar evolution.

References

[1] F. Hoyle, Astrophys. J. Suppl. Ser. 1, 121 (1954).
[2] E.E. Salpeter, Astrophys. J. **115**, 326 (1952).
[3] M. Katsuma, Phys. Rev. C **78**, 034606 (2008); Astrophys. J. **745**, 192 (2012); Springer Proc. in Physics **219**, 389 (2019); JPS Conf. Proc. **31**, 011060 (2020).
[4] D. Dell'Aquila, *et al.*, Phys. Rev. Lett. **119**, 132501 (2017); R. Smith, *et al.*, Phys. Rev. Lett. **119**, 132502 (2017).
[5] C. Angulo, M. Arnould, *et al.*, Nucl. Phys. A **656**, 3 (1999).
[6] G.R. Caughlan, W.A. Fowler, At. Data Nucl. Data Tables **40**, 283 (1988).
[7] K. Nomoto, F.-K. Thielemann, S. Miyaji, Astron. Astrophys. **149**, 239 (1985).
[8] K. Langanke, M. Wiescher, F.-K. Thielemann, Z. Phys. A **324**, 147 (1986).
[9] P. Descouvemont, D. Baye, Phys. Rev. C **36**, 54 (1987).
[10] D.V. Fedorov, A.S. Jensen, Phys. Lett. B **389**, 631 (1996).
[11] S. Ishikawa, Phys. Rev. C **87**, 055804 (2013); ibid. **90**, 061604 (2014).
[12] H. Suno, Y. Suzuki, P. Descouvemont, Phys. Rev. C **94**, 054607 (2016).
[13] N.B. Nguyen, F.M. Nunes, I.J. Thompson, Phys. Rev. C **87**, 054615 (2013); N.B. Nguyen, F.M. Nunes, I.J. Thompson, E.F. Brown, Phys. Rev. Lett., **109** , 141101 (2012); N.B. Nguyen, Ph.D. dissertation, Michigan State University (2013).
[14] I.J. Thompson, F.M. Nunes, *Nuclear Reactions for Astrophysics*, (Cambridge University Press, 2009).
[15] P. Descouvemont, J. Phys. G **37**, 64010 (2010); *Theoretical Models for Nuclear Astrophysics*, (Nova Science Publishers, 2003).
[16] M. Katsuma, Y. Sakuragi, S. Okabe, Y. Kondō, Prog. Theor. Phys. **107**, 377 (2002).
[17] G.R. Satchler, *Direct Nuclear Reactions*, (Oxford University Press, 1983)
[18] S. Ali, A.R. Bodmer, Nucl. Phys. **80**, 99 (1966).
[19] B. Buck, H. Friedrich, C. Wheatley, Nucl. Phys. A **275**, 246 (1977); G.R. Satchler, W.G. Love, Phys.Rep. **55**, 183 (1979); G. Bertsch, J. Borysowicz, H. McManus, W.G. Love, Nucl. Phys. A **284**, 399 (1977).
[20] D. Baye, Phys. Rev. Lett. **58**, 2738 (1987).
[21] International Network of Nuclear Reaction Data Centres, EXFOR, Experimental Nuclear Reaction Data.
[22] J.H. Kelley, J.E. Purcell, C.G. Sheu, Nucl. Phys. A **968**, 71 (2017).

mkatsuma@gmail.com